Age of Information for Wireless Energy Harvesting Secondary Users in Cognitive Radio Networks

Shiyang Leng*, Xiaoyong Ni†, and Aylin Yener*

*Department of Electrical Engineering, The Pennsylvania State University, University Park, PA, USA
†Glasgow College, University of Electronic Science and Technology of China, Chengdu, China
sfl5154@psu.edu *nixiaoyong@std.uestc.edu.cn* *yener@engr.psu.edu*

***Abstract*—Age of information (AoI) is recently introduced to serve as a performance metric that quantifies the freshness of information for wireless applications with time-sensitive data. This paper studies AoI of wireless energy harvesting nodes in a multiuser cognitive radio network. In the envisioned network, primary users (PUs) and secondary users (SUs) coexist in such way that SUs harvest wireless energy from active PUs and access the primary spectrum opportunistically to transmit status updates. We model the distributions of PUs and SUs by a homogeneous Poisson point process and a binomial point process, respectively. We consider a greedy policy where each SU transmits an update whenever it harvests sufficient energy. A nonlinear energy harvesting model is used for SUs. Under the greedy policy, the average AoI of the secondary network is analyzed. An upper bound and a lower bound of the average AoI are derived. Simulation results demonstrate that the bounds closely approximate the average AoI.**

***Keywords*-age of information; cognitive radio networks; wireless energy harvesting.**

I. Introduction

Contemporary and forthcoming wireless applications, e.g., vehicular networks and unmanned aerial vehicles networks, necessitate frequent information exchange between nodes. Requirements for such networks include, for example, periodically updating information among peer nodes on a short timescale in order to convey the states of dynamic processes of the underlying system. Age of information (AoI) [1] is an appropriate performance metric to quantify the freshness of such status updates. AoI measures the time elapsed since the generation of the latest successfully received update. Different from the traditional metric of delay, AoI thus captures the timeliness of the received information from the destination's perspective.

AoI has been widely studied in various system setups, after its introduction in the context of vehicular networks [2]. Its characteristics are then analyzed using queueing theory in [3] for first-come-first-served (FCFS) queues. Last-come-first-served (LCFS) service is considered in [4]. References [5] and [6] consider AoI in broadcast and multi-hop networks, respectively. An AoI penalty function which generalizes linear and nonlinear models of age is introduced in [7] and the optimality condition is found for the zero-wait policy. Update policy for AoI minimization in multicast networks is studied in [8], [9]. In [10], multiple updating sources sharing one server are considered and AoI for FCFS and LCFS queues are evaluated. User scheduling problems are studied for broadcast networks in [11], [12]. In [13], [14], scheduling update requests of multiple users is investigated and maximum-age-first scheduling strategies are shown to be optimal.

AoI for energy harvesting communication systems has recently been studied in a series of works, see [15]–[27]. In these systems, each status update consumes harvested energy, and AoI minimization taking into account the intermittency of energy is of interest. Update policies for an energy harvesting node have been investigated in [15] under the energy causality constraint. The results show that an optimal policy is lazy, leaving a certain idle period between updates instead of transmitting as frequently as possible. References [16], [17] consider a single-hop model for offline and online schedules. Reference [18] considers AoI in a two-hop network. The optimal update policy is derived by relating to the solution of the single-hop model. In [19], asymptotically optimal update policies for infinite, finite, and unit battery size are derived. For a unit battery, the optimal policy is proved to be a threshold policy. Reference [20] considers full battery recharge and incremental battery recharge models for a finite battery. In the class of renewal policies, the optimal policy is proved to show an energy-dependent multi-threshold structure. Reference [21] proposes a model where information is conveyed by timings of the updates and studies the tradeoff between the achievable information rate and achievable average AoI. References [22], [23] consider update failures due to the noisy channel. A non-linear function of AoI is analyzed in [24] considering randomness in update generation, transmission, and energy arrival. Moreover, AoI in wireless powered networks, where nodes obtain energy from dedicated wireless energy sources, has been considered in [25]–[27].

More recently, AoI has been considered in cognitive radio networks (CRNs) [28]–[31]. In particular, in [29], the optimal sensing and updating policies for energy harvesting secondary users (SUs) are investigated to minimize the average AoI. A model of partially observable Markov decision process (POMDP) is established to make sequential decisions based on energy harvesting and channel states. It is proved that the optimal policy has a threshold structure in terms of energy state and AoI. In these works, the interaction between primary users (PUs) and SUs is considered only for spectrum access,

2155-6814/19/$31.00 ©2019 IEEE
DOI 10.1109/MASS.2019.00049

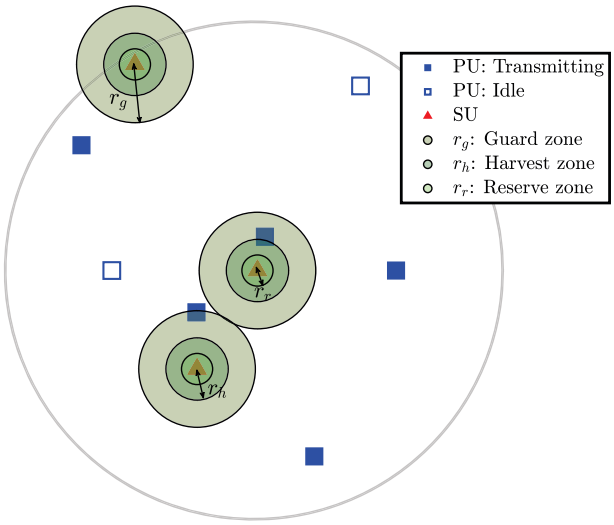

Figure 1. System model.

and the energy source of SUs is not specified. In fact, SUs can harvest RF energy from ambient PUs in CRNs [32], in which case the activities of PUs will impact the state of SUs and their AoI. Specifically, as the probability of activity and the transmission power of PUs increase, the SUs will have a more abundant energy source to harvest from, but will experience a poorer channel. In other words, PUs serve as both energy sources and interferers that block potential transmissions from SUs' perspective.

Considering this trade-off, in this paper, we investigate the AoI of SUs and identify the impact of the underlying primary network. In particular, we model the primary network by a homogeneous Poisson point process (HPPP) as in previous work on energy harvesting cognitive radio networks (EH-CRNs) [32], [33]. The SUs are considered to follow a binomial point process (BPP) with a fixed number of nodes in a finite area. To protect the transmissions of PUs and to avoid interference caused by PUs, each SU transmits only when no PUs appear in the associated *guard zone* [32], [33]. We apply a nonlinear energy harvesting model and take into account the sensitivity and saturation properties of wireless energy harvesting from RF signals. We first derive the outage probability of PUs and then focus on investigating the AoI of the secondary network using a greedy update policy, which is easy to implement in practical applications. Specifically, each SU transmits an update whenever it harvests enough energy [25], [26]. We derive an upper and a lower bound to approximate the average AoI. Simulations demonstrate that the approximation is close to the real average AoI.

II. System Model

A. Network Model

We consider a cognitive radio network, where primary users (PUs) and secondary users (SUs) are distributed in a disk of radius R, as shown in Fig. 1. Time is slotted with slot length normalized to 1. PUs are distributed as an HPPP with density $\lambda'_{\rm p}$. Each PU accesses the spectrum independently with probability ρ in each slot, thus, the active PUs form another HPPP with density $\lambda_{\rm p} = \rho\lambda'_{\rm p}$ [32]. In the rest of the paper, only the point process of active PUs is involved, thus, we simply refer to active PUs as PUs. SUs are placed in the area independently and uniformly, which are distributed as a BPP with a fixed number of nodes $N_{\rm s}$. The point processes of PUs and SUs are denoted as $\Phi_{\rm p} = \{x\}$ and $\Phi_{\rm s} = \{y\}$, where $x, y \in \mathbb{R}^2$ are the coordinates of PUs and SUs, respectively. The point processes vary independently over slots. All PUs are connected to the power-grid and transmit to the primary receivers (PRs) with fixed power $P_{\rm p}$. Each PR is placed $d_{\rm p}$ meters away from its PU in a random direction. SUs harvest energy from the RF signals of PUs. The harvested energy of an SU is used to generate status updates and send them to its intended secondary receiver (SR). Each SU is either harvesting energy or transmitting updates in a slot. It transmits with fixed power $P_{\rm s}$ to its SR in a distance $d_{\rm s}$. We assume $d_{\rm s} \ll R$ and $P_{\rm s} \ll P_{\rm p}$ for the interest of practical wireless energy harvesting applications.

We consider a flat-fading channel with small-scale Rayleigh fading and large-scale path loss. In each time slot, the channel coefficient, g_x, for the channel between the PU at x and the receiver at the origin is an exponential random variable with unit mean, i.e., $g_x \sim \text{Exp}(1)$. Similarly, the channel coefficient for the SU is $g_y \sim \text{Exp}(1)$. The coefficients $\{g_x\}_{x\in\Phi_{\rm p}}$ and $\{g_y\}_{y\in\Phi_{\rm s}}$ are independent and identically distributed (i.i.d.). The path loss for PUs and SUs are $|x|^{-\alpha}$ and $|y|^{-\alpha}$, respectively, where $|\cdot|$ denotes the Euclidean distance to the origin and $\alpha \geq 2$ is the path loss exponent.

B. Transmission Model

The SUs transmits to the intended SRs by opportunistically accessing the spectrum of the primary network. To guarantee the quality of service (QoS) of PUs, an SU is not allowed to transmit if there are PRs in the neighborhood of the SU. We consider a *guard zone* $\mathcal{B}(y, r_{\rm g})$, which is defined as a disk centered at the SU located at y with radius $r_{\rm g}$. The SU is allowed to transmit only if the number of PRs in the guard zone, denoted by $N_{\rm g}$, is zero. The radius $r_{\rm g}$ is determined according to the SU's power $P_{\rm s}$ and the QoS of PUs. Recall that each PR is separated from its PU by a distance of $d_{\rm p}$ in a random direction. By the homogeneity of the HPPP and the displacement theorem [34], the placement of PRs can be considered to be an HPPP with density $\lambda_{\rm p}$. Thus, $N_{\rm g}$ is a Poisson random variable with mean $\pi r_{\rm g}^2\lambda_{\rm p}$. The probability that an SU has a clear guard zone is given by

$$\rho_{\rm g} = \Pr(N_{\rm g} = 0) = \exp(-\pi r_{\rm g}^2\lambda_{\rm p}). \tag{1}$$

For a receiver at the origin, the aggregate interference caused by PUs is given by

$$I_{\rm p} = \sum_{x\in\Phi_{\rm p}} P_{\rm p} g_x |x|^{-\alpha}. \tag{2}$$

Note that due to the homogeneity of PPP, it does not matter where $I_{\rm p}$ is measured and $I_{\rm p}$ is the same for a PR and an SR [32]. However, for the BPP of SUs, the interference caused by the secondary network seen by a receiver in the center of the network is different from that at the network boundary, which is location dependent [35]. Let $I_{\rm s1}$ and $I_{\rm s2}$ denote the aggregate interference caused by SUs at a PR and an SR, respectively. For a certain PR at x_0 with the associated PU at $x_{\rm p}$,

$$I_{\rm s1} = \sum_{y \in \Phi_{\rm s}} P_{\rm s} \mathbb{1}_y g_y \left| y - x_0 \right|^{-\alpha}, \tag{3}$$

where $\mathbb{1}_y$ denote the indicator of the event that the SU at y transmits, and $\rho_{\rm t} \triangleq \Pr(\mathbb{1}_y = 1)$. For an SR located at y_0 with the associated SU at $y_{\rm s}$, we have

$$I_{\rm s2} = \sum_{y \in \Phi_{\rm s} \setminus y_{\rm s}} P_{\rm s} \mathbb{1}_y g_y \left| y - y_0 \right|^{-\alpha}. \tag{4}$$

The received signal-to-interference-plus-noise ratios (SINRs) at a PR and an SR are given by

$$\gamma_{\rm p} = \frac{P_{\rm p} g_{x_{\rm p}} d_{\rm p}^{-\alpha}}{I_{\rm p} + I_{\rm s1} + \sigma^2}, \tag{5}$$

$$\gamma_{\rm s} = \frac{P_{\rm s} g_{y_{\rm s}} d_{\rm s}^{-\alpha}}{I_{\rm p} + I_{\rm s2} + \sigma^2}, \tag{6}$$

where σ^2 is the additive white Gaussian noise (AWGN) power.

C. Energy Harvesting Model

Each SU harvests RF energy from PUs signals and charges a finite-capacity battery before use. The battery capacity is denoted by $\bar{b}$. SUs convert the received RF signal to energy and store it in the battery. The received power of an SU at the origin in slot t is given by

$$P_{\rm r}(t) = \sum_{x \in \Phi_{\rm p}} P_{\rm p} g_x \left| x \right|^{-\alpha}. \tag{7}$$

In practice, the power conversion circuit has a sensitivity requirement and a saturation region [36]. When the received power is below the sensitivity threshold, the output DC power is zero, and when the received power is higher than the saturation threshold, the output power is a constant. In between, the output power is approximated to increase linearly. We apply a simplified model for the output power:

$$P_{\rm o}(t) = \begin{cases} 0, & \text{if } P_{\rm r}(t) \le \epsilon_1, \\ \eta P_{\rm r}(t), & \text{if } \epsilon_1 < P_{\rm r}(t) \le \epsilon_2, \\ \bar{P}, & \text{if } P_{\rm r}(t) > \epsilon_2, \end{cases} \tag{8}$$

where $0 < \eta < 1$ is the energy conversion efficiency, and ϵ_1, ϵ_2 are the sensitivity and saturation thresholds.

Due to the fact that the received power is dominated by the transmission power and the path loss, we define the *harvest zone* $\mathcal{B}(y, r_{\rm h})$, which is a disk centered at an SU located at y [32]. The radius $r_{\rm h}$ of the harvest zone is determined by the sensitivity threshold ϵ_1, transmission power $P_{\rm p}$, and PUs' density $\lambda_{\rm p}$, such that it is reasonable to assume that the SU harvests nonzero energy only from the PUs located in the harvest zone. The received power from PUs outside the harvest zone is approximated to be smaller than ϵ_1, thus, assumed to be negligible. We denote the probability that an SU has a nonzero output power by $\rho_{\rm h}$, which is equal to the probability that at least one PU is inside the harvest zone. Note that the number of PUs inside the harvest zone, denoted by $N_{\rm h}$, is a Poisson random variable with mean $\pi r_{\rm h}^2 \lambda_{\rm p}$. Thus, $\rho_{\rm h}$ is given by

$$\rho_{\rm h} = \Pr(N_{\rm h} \ge 1) = 1 - \exp(-\pi r_{\rm h}^2 \lambda_{\rm p}). \tag{9}$$

Similarly, we also define the *reserve zone* $\mathcal{B}(y, r_{\rm r})$ as a disk centered at y with the radius $r_{\rm r}$ chosen based on $\bar{P}$, $P_{\rm p}$, ϵ_2, and $\lambda_{\rm p}$. The harvested power from PUs in the reserve zone is approximated to be the saturation power $\bar{P}$. Consequently, the harvested power of an SU at the origin can be expressed as

$$P_{\rm o}(t) = \sum_{x \in \mathcal{D}_1} \eta P_{\rm p} g_x \left| x \right|^{-\alpha} + \sum_{x \in \mathcal{D}_2} \bar{P}, \tag{10}$$

where $\mathcal{D}_1 = \{x : x \in \Phi_{\rm p}, x \in \mathcal{B}((0,0), r_{\rm h}) \backslash \mathcal{B}((0,0), r_{\rm r})\}$, and $\mathcal{D}_2 = \{x : x \in \Phi_{\rm p}, x \in \mathcal{B}((0,0), r_{\rm r})\}$. The battery state at the beginning of slot t, i.e., the end of slot $t-1$, evolves as

$$b(t) = \min\Big\{ b(t-1) - a(t)E + (1 - a(t)) P_{\rm o}(t), \bar{b} \Big\}, \tag{11}$$

where E denotes the energy consumed to generate and send an update, and $a(t)$ is a binary variable representing whether the SU transmits or not. Specifically, $a(t) = 1$ indicates the SU generates an update and transmits, and $a(t) = 0$ indicates the SU does not update but harvests energy.

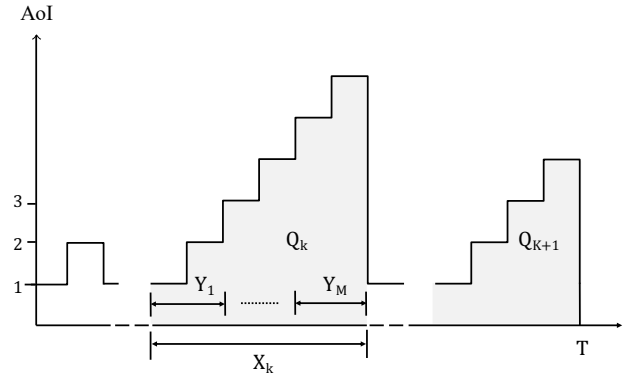

Figure 2. A sample path of AoI.

D. Performance Metrics

We consider the outage probability to measure the performance of PUs. That is $p_{\rm out} = \Pr(\gamma_{\rm p} < \theta_{\rm p})$, where $\theta_{\rm p}$ is the required SINR at PRs. For the secondary network, we evaluate the performance metric, namely, average AoI for SUs. A linear model of AoI is used, where AoI is defined as the time duration between the current time t and the generation instant of the most recent received update by t. Specifically, the AoI of status updates of an SU is given by

$$\Delta(t) = t - u(t), \tag{12}$$

where $u(t)$ is the generation time of the most recent received update by t. We consider a traget SINR $\theta_{\rm s}$ for the received signal at an SR. An update is said to be successful if $\gamma_{\rm s} \geq \theta_{\rm s}$ such that the update information can be decoded correctly. As shown in Fig. 2, the AoI increases between successful updates. Here, we consider updates are generated at will and transmitting an update takes one slot. This means that upon each transmission, the SU generates a new data packet containing the information of current status. Thus, the AoI drops to 1 when the SU successfully sends an update. Specifically, at the beginning of a slot,

$$\Delta(t+1) = \begin{cases} 1, & \text{if an update succeeds,} \\ \Delta(t)+1, & \text{otherwise.} \end{cases} \tag{13}$$

The long-term average AoI for an SU is given by

$$\Delta = \lim_{T\to\infty} \sum_{t=1}^{T} \Delta(t). \tag{14}$$

III. Outage Probability of Primary Network

We first consider the outage probability of the primary network, which is given by

$$p_{\rm out} = \Pr\Big(\frac{P_{\rm p} g_{x_{\rm p}} d_{\rm p}^{-\alpha}}{I_{\rm p} + I_{\rm s1} + \sigma^2} < \theta_{\rm p} \Big). \tag{15}$$

We provide the expression of $p_{\rm out}$ in the following theorem.

Theorem 1: The outage probability of a PU is given by

$$p_{\rm out} = 1 - \exp(-\phi_1)(1 - \rho_{\rm t} + \rho_{\rm t}\phi_2)^{N_{\rm s}} \tag{16}$$

where

$$\phi_1 = \frac{\theta_{\rm p} d_{\rm p}^{\alpha} \sigma^2}{P_{\rm p}} + \frac{\pi \lambda_{\rm p} \theta_{\rm p}^{\frac{2}{\alpha}} d_{\rm p}^2}{\mathrm{sinc}(\frac{2}{\alpha})}, \tag{17}$$

$\rho_{\rm t}$ is specified later in (47), and ϕ_2 is given by (63) in Appendix A.

The proof of Theorem 1 is given in Appendix A.

IV. AoI of Secondary Network

In this section, we apply a greedy policy for status updates, which is simple for practical implementations. By the greedy policy, each SU generates and sends an update at slot t whenever it has harvested energy at least E by the end of slot $t-1$ and has a clear guard zone at slot t. The policy is formally defined as follows.

Definition 1: The greedy policy Ω_1 is given by

$$\Omega_1 : a(t) = \begin{cases} 1, & \text{if and only if } b(t) \geq E,\ N_{\rm g}(t) = 0, \\ 0, & \text{otherwise.} \end{cases} \tag{18}$$

We further assume that the battery capacity $\bar{b}$ is equal to E. Equivalently, the battery is depleted by every update operation [25], [26]. Under this assumption, we derive the upper and lower bounds for the long-term average AoI.

A. Analysis of AoI

Let X_k denote the number of slots between the $(k-1)$-th and k-th successfully received updates. The interval between two consecutive transmissions is denoted by Y_m, where $m = 1, 2, \ldots, M$, and M denotes the number of transmissions for a successful update. Note that M is a geometic random variable with $\rho_{\rm u}$, the probability that an SU succeeds to update in a slot. X_k and Y_m are i.i.d. random variables in terms of k and m, respectively. In particular,

$$X_i = \sum_{m=1}^{M} Y_m. \tag{19}$$

For a period of T slots, during which K updates have been successfully delivered, the average AoI is given by

$$\Delta_T = \frac{1}{T}\sum_{k=1}^{K+1} Q_k = \frac{K}{T}\frac{1}{K}\sum_{k=1}^{K} Q_k + \frac{1}{T} Q_{K+1}, \tag{20}$$

where Q_k is the area between the $(k-1)$-th and k-th successful updates, cf. Fig. 2, which is given by

$$Q_k = \sum_{i=1}^{X_k} i = \frac{1}{2} X_k (X_k + 1). \tag{21}$$

Note that as T goes to infinity, K goes to infinity, thus

$$\lim_{T\to\infty} \frac{K}{T} = \frac{1}{\mathbb{E}[X]}, \tag{22}$$

$$\lim_{K\to\infty} \frac{1}{K}\sum_{k=1}^{K} Q_k = \mathbb{E}[Q] \tag{23}$$

almost surely. Also, Q_{k+1}/T goes to zero as T grows. Thus, we have the long-term average AoI

$$\Delta = \lim_{T\to\infty} \Delta_T = \frac{\mathbb{E}[X^2]}{2\mathbb{E}[X]} + \frac{1}{2}. \tag{24}$$

From (19), we have

$$\mathbb{E}[X] = \mathbb{E}_M\Big[\mathbb{E}_Y\Big[\sum_{m=1}^{M} Y_m\Big]\Big] = \mathbb{E}[M]\mathbb{E}[Y] = \mathbb{E}[Y]/\rho_{\rm u} \tag{25}$$

$$\mathbb{E}[X^2] = \mathbb{E}_M\Big[\mathbb{E}_Y\Big[\sum_{m=1}^{M} Y_m^2 + \sum_{m=1}^{M}\sum_{k\neq m}^{M} Y_m Y_j\Big]\Big] \tag{26}$$

$$= \mathbb{E}[M]\mathbb{E}[Y^2] + (\mathbb{E}[M^2] - \mathbb{E}[M])\mathbb{E}[Y]^2 \tag{27}$$

$$= \frac{1}{\rho_{\rm u}}\mathbb{E}[Y^2] + \frac{2(1-\rho_{\rm u})}{\rho_{\rm u}^2}\mathbb{E}[Y]^2 \tag{28}$$

By substituting (25) and (28) into (24), Δ can be written as

$$\Delta = \frac{\mathbb{E}[Y^2]}{2\mathbb{E}[Y]} + \frac{1-\rho_{\rm u}}{\rho_{\rm u}}\mathbb{E}[Y] + \frac{1}{2}. \tag{29}$$

Between two consecutive transmissions, an SU first accumulates energy up to E, then waits for a clear guard zone. Let e_l denote the harvested energy over l slots, i.e., $e_l = \sum_{t=1}^{l} P_{\rm o}(t)$. Let L be the random variable denoting the number of slots an

SU takes to fully charge its battery. Then, the mean of Y is derived as follows.

$$\mathbb{E}[Y] = \sum_{k=1}^{\infty} k\Pr(Y=k) \tag{30}$$

$$= \sum_{k=1}^{\infty} k \sum_{l=1}^{k} \Pr(e_{l-1} < E, e_l \geq E)(1-\rho_{\rm g})^{k-l}\rho_{\rm g} \tag{31}$$

$$= \sum_{l=1}^{\infty} \Pr(e_{l-1} < E, e_l \geq E) \sum_{k\geq l}^{\infty} k(1-\rho_{\rm g})^{k-l}\rho_{\rm g} \tag{32}$$

$$= \sum_{l=1}^{\infty} \Pr(e_{l-1} < E, e_l \geq E) \sum_{i=0}^{\infty} (i+l)(1-\rho_{\rm g})^{i}\rho_{\rm g} \tag{33}$$

$$= \sum_{l=1}^{\infty} \Pr(e_{l-1} < E, e_l \geq E) \Big(\frac{1-\rho_{\rm g}}{\rho_{\rm g}} + l\Big) \tag{34}$$

$$= \mathbb{E}[L] + \frac{1-\rho_{\rm g}}{\rho_{\rm g}}, \tag{35}$$

where $\rho_{\rm g}$ is given in (1). Similarly, the second-order moment of Y can be written as

$$\mathbb{E}[Y^2] = \sum_{l=1}^{\infty} \Pr(e_{l-1} < E, e_l \geq E) \sum_{k\geq l}^{\infty} k^2(1-\rho_{\rm g})^{k-l}\rho_{\rm g} \tag{36}$$

$$= \mathbb{E}[L^2] + \frac{2(1-\rho_{\rm g})}{\rho_{\rm g}}\mathbb{E}[L] + \frac{1-\rho_{\rm g}}{\rho_{\rm g}^2}. \tag{37}$$

Next, we focus on characterizing the full charging time L and the successful update probability $\rho_{\rm u}$.

B. Full Charging Time

We first identify the average harvested energy in one slot at an SU. Due to the finite battery, the harvested power at each slot is at most $\min\{P_{\rm o}(t), \bar{b}\}$, where $P_{\rm o}(t)$ is given in (10). Considering practical wireless energy harvesting applications, the harvested energy per slot is usually far less than the battery capacity such that it takes a number of slots to fully charge the battery. Thus, we assume $P_{\rm o}(t) \ll \bar{b}$ for all t, and characterize the harvested energy per slot in the following lemma.

Lemma 1: The mean and variance of the harvested energy per slot by an SU is given by

$$\mathbb{E}[P_{\rm o}] = \pi\lambda_{\rm p}\Big[r_{\rm r}^2\bar{P} + \frac{2\eta P_{\rm p}}{2-\alpha}\big(r_{\rm h}^{2-\alpha} - r_{\rm r}^{2-\alpha}\big)\Big], \tag{38}$$

$$\mathrm{Var}(P_{\rm o}) = \pi\lambda_{\rm p} r_{\rm r}^2\bar{P}^2 + \frac{2\pi\lambda_{\rm p}\eta^2 P_{\rm p}^2}{1-\alpha}\big(r_{\rm h}^{2-2\alpha} - r_{\rm r}^{2-2\alpha}\big) + \frac{4\pi^2\lambda_{\rm p}^2\eta^2 P_{\rm p}^2}{(2-\alpha)^2}\big(r_{\rm h}^{2-\alpha} - r_{\rm r}^{2-\alpha}\big)^2. \tag{39}$$

The proof of Lemma 1 is given in Appendix B.

In the i-th charging cycle, it takes L_i slots to accumulate energy, i.e.,

$$\sum_{t=1}^{L_i} P_{\rm o}(t) \geq E, \quad \sum_{t=1}^{L_i-1} P_{\rm o}(t) < E. \tag{40}$$

Then, taking expectation on both sides results in

$$\mathbb{E}\Big[\sum_{t=1}^{L_i} P_{\rm o}(t)\Big] = \mathbb{E}[L]\mathbb{E}[P_{\rm o}] \geq E \tag{41}$$

$$\mathbb{E}\Big[\sum_{t=1}^{L_i-1} P_{\rm o}(t)\Big] = (\mathbb{E}[L]-1)\mathbb{E}[P_{\rm o}] < E. \tag{42}$$

Thus, the expected time to fully charge the battery is given by

$$\mathbb{E}[L] = \Big\lceil \frac{E}{\mathbb{E}[P_{\rm o}]} \Big\rceil. \tag{43}$$

Further, we can derive based on (40) and (41) that

$$\mathbb{E}\Big[\Big(\sum_{t=1}^{L_i-1} P_{\rm o}(t)\Big)^2\Big] < E\mathbb{E}\Big[\sum_{t=1}^{L_i-1} P_{\rm o}(t)\Big]] \tag{44}$$

$$\leq \mathbb{E}[L]\mathbb{E}[P_{\rm o}]\mathbb{E}\Big[\sum_{t=1}^{L_i-1} P_{\rm o}(t)\Big]]. \tag{45}$$

The LHS is $(\mathbb{E}[L]-1)\mathbb{E}[P_{\rm o}^2] + (\mathbb{E}[L^2]-3\mathbb{E}[L]+2)\mathbb{E}[P_{\rm o}]^2$ and the RHS is $\mathbb{E}[L](\mathbb{E}[L]-1)\mathbb{E}[P_{\rm o}]^2$. Since $\mathbb{E}[L]^2 \leq \mathbb{E}[L^2]$ and $\mathbb{E}[P_{\rm o}]^2 \leq \mathbb{E}[P_{\rm o}^2]$, the upper and lower bound of $\mathbb{E}[L^2]$ can be obtained by

$$\mathbb{E}[L]^2 \leq \mathbb{E}[L^2] \leq \mathbb{E}[L]^2 + \mathbb{E}[L] - 1. \tag{46}$$

C. Successful Update Probability

By the definition of the greedy update policy, transmission probability $\rho_{\rm t}$ is equal to the probability that the SU has fully charged the battery by the end of a slot and has a clear guard zone in the next slot. Since the point processes vary independently over slots, the energy harvesting state in one slot and the guard zone state in the next slot are independent. Thus, the transmission probability is simply given by

$$\rho_{\rm t} = \rho_{\rm f}\rho_{\rm g} = \frac{\rho_{\rm g}}{\mathbb{E}[L]}, \tag{47}$$

where $\rho_{\rm f}$ denotes the full charging probability in a slot. Given that the SU transmits in a slot, successful update probability $\rho_{\rm u}$ is defined as a conditional probability, that is

$$\rho_{\rm u} \triangleq \Pr(\gamma_{\rm s} \geq \theta_{\rm s} | N_{\rm g} = 0). \tag{48}$$

We characterize $\rho_{\rm u}$ in the following lemma.

Lemma 2: The successful update probability for a transmitting SU is approximated by

$$\rho_{\rm u} \approx \min\Big\{1, \frac{1}{\rho_{\rm g}}\exp(-\beta_1)(1-\rho_{\rm t}+\rho_{\rm t}\beta_2)^{N_{\rm s}-1}\Big\} \tag{49}$$

where

$$\beta_1 = \frac{\theta_{\rm s} d_{\rm s}^{\alpha}\sigma^2}{P_{\rm s}} + \frac{\lambda_{\rm p}\pi}{\mathrm{sinc}(\frac{2}{\alpha})}\Big(\frac{\theta_{\rm s} d_{\rm s}^{\alpha} P_{\rm p}}{P_{\rm s}}\Big)^{\frac{2}{\alpha}}, \tag{50}$$

$\rho_{\rm t}$ and β_2 are given by (47) and (77), respectively.

The proof of Lemma 2 is given in Appendix C.

Table I
SIMULATION PARAMETERS.

Area radius R	50 m
Number of SUs N_s	80
Guard zone radius r_g	4 m
Harvesting zone radius r_h	3 m
Energy conversion efficiency η	0.1
Noise power σ^2	-114 dBm
Target SINR θ_p, θ_s	5

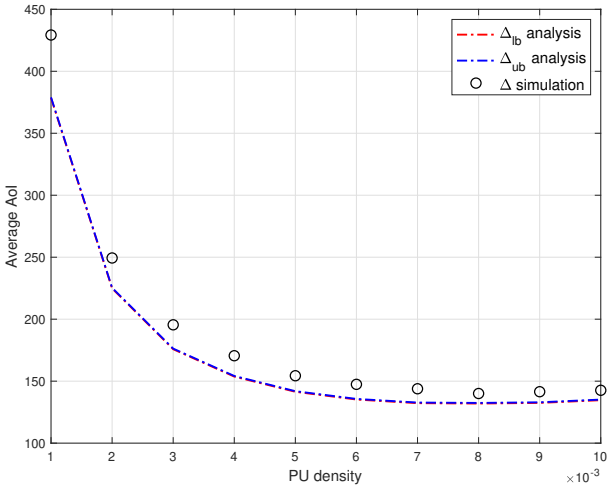

Figure 3. Average AoI vs. PU density with $\alpha = 3.5$, $r_r = 1.5$, $P_p = 1$, $P_s = 0.2$, $d_p = d_s = 2$.

Consequently, after some arrangement, we can obtain an upper and a lower bound for the average AoI, i.e., $\Delta_{lb} \leq \Delta \leq \Delta_{ub}$,

$$\Delta_{lb} = \frac{\mathbb{E}[L]^2}{2\left(\mathbb{E}[L] + \frac{1-\rho_g}{\rho_g}\right)} + \frac{1-\rho_u}{\rho_u}\left(\mathbb{E}[L] + \frac{1-\rho_g}{\rho_g}\right) + \frac{1}{2}, \tag{51}$$

$$\Delta_{ub} = \frac{\mathbb{E}[L]^2 + \mathbb{E}[L] - 1}{2\left(\mathbb{E}[L] + \frac{1-\rho_g}{\rho_g}\right)} + \frac{1-\rho_u}{\rho_u}\left(\mathbb{E}[L] + \frac{1-\rho_g}{\rho_g}\right) + \frac{1}{2}, \tag{52}$$

where $\mathbb{E}[L]$ can be obtained by (43) and Lemma 1, ρ_g and ρ_u are given in (1) and Lemma 2, respectively.

V. SIMULATION

In this section, we provide simulation results and compare them with the analytical derivations. The fixed parameters are listed in Table I. Results on average AoI, average full charging time, outage probability, and successful update probability are illustrated in the following figures.

Fig. 3-5 show the results when varying PUs' density λ_p with $\alpha = 3.5$, $r_r = 1.5$, $P_p = 1$, $P_s = 0.2$, $d_p = d_s = 2$. It can be observed in Fig. 3 that the analytical result closely approximates the simulated average AoI. The average AoI achieves the minimum at $\lambda_p = 0.008$ in this setting since varying the

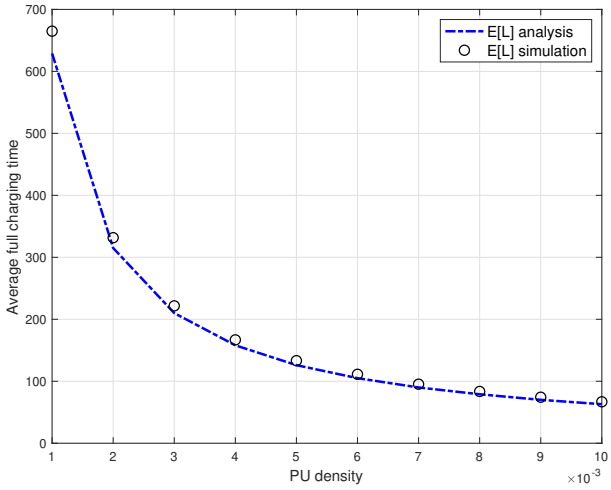

Figure 4. Average of full charging time vs. PU density with $\alpha = 3.5$, $r_r = 1.5$, $P_p = 1$, $P_s = 0.2$, $d_p = d_s = 2$.

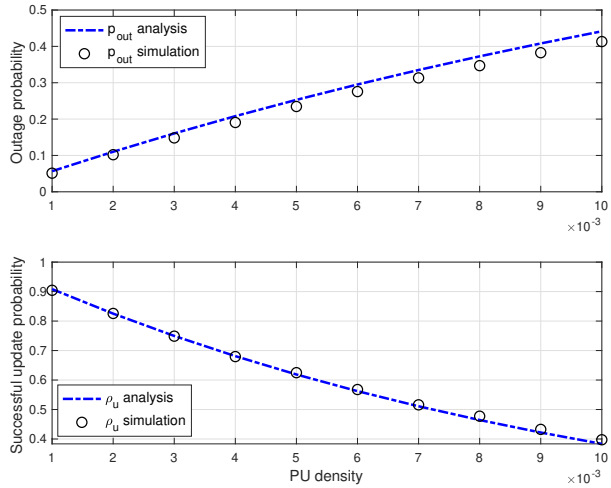

Figure 5. Probabilities vs. PU density with $\alpha = 3.5$, $r_r = 1.5$, $P_p = 1$, $P_s = 0.2$, $d_p = d_s = 2$.

density of PUs causes a trade-off between energy harvesting and successfully updating. As the density of PUs increases, the full charging time $\mathbb{E}[L]$ decreases sharply as shown in Fig. 4 since more PUs are serving as energy sources. The decreasing $\mathbb{E}[L]$ results in the decrease of average AoI. On the other hand, the successful update probability of SUs decreases because a larger interference is caused by an increasing number of PUs, cf. Fig. 5. At the same time, the outage probability of PUs increases not only due to the more intense interference from PUs but also the increasing interference from SUs, which is caused by the more frequent update transmissions as the full charging time becomes smaller.

In Fig. 6 and Fig. 7, we vary the transmit power of SUs

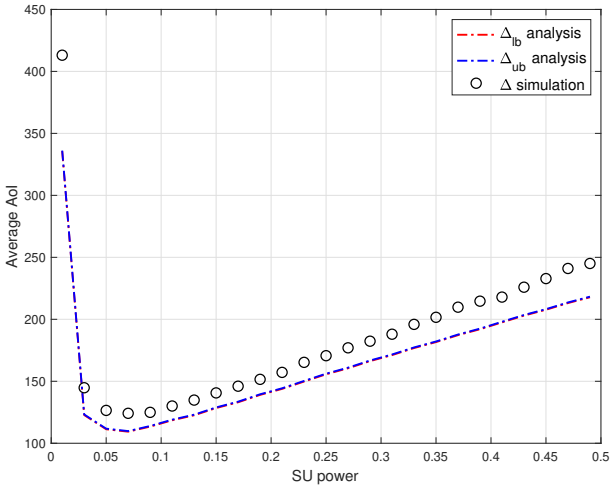

Figure 6. Average AoI vs. SU power with $\alpha = 3.5$, $r_{\mathrm{r}} = 1.5$, $P_{\mathrm{p}} = 1$, $\lambda_{\mathrm{p}} = 0.005$, $d_{\mathrm{p}} = d_{\mathrm{s}} = 2$.

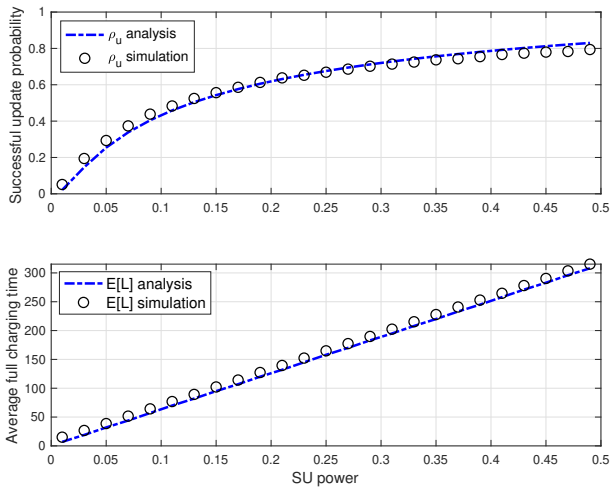

Figure 7. Successful update probability and average full charging time vs. SU power with $\alpha = 3.5$, $r_{\mathrm{r}} = 1.5$, $P_{\mathrm{p}} = 1$, $\lambda_{\mathrm{p}} = 0.005$, $d_{\mathrm{p}} = d_{\mathrm{s}} = 2$.

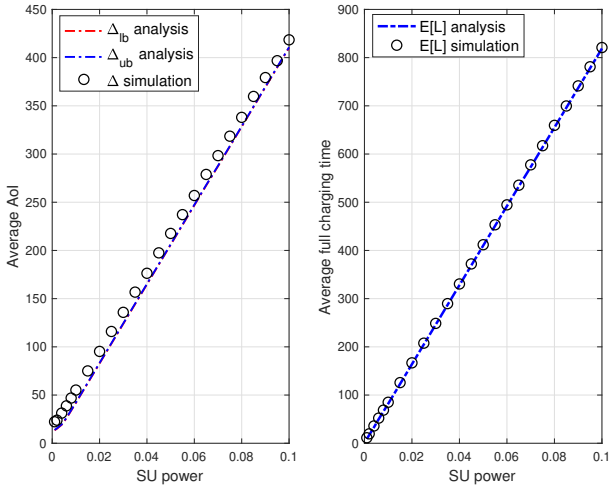

Figure 8. Average AoI vs. SU power with $\alpha = 4$, $r_{\mathrm{r}} = 2$, $P_{\mathrm{p}} = 0.1$, $\lambda_{\mathrm{p}} = 0.01$, $d_{\mathrm{p}} = d_{\mathrm{s}} = 1$.

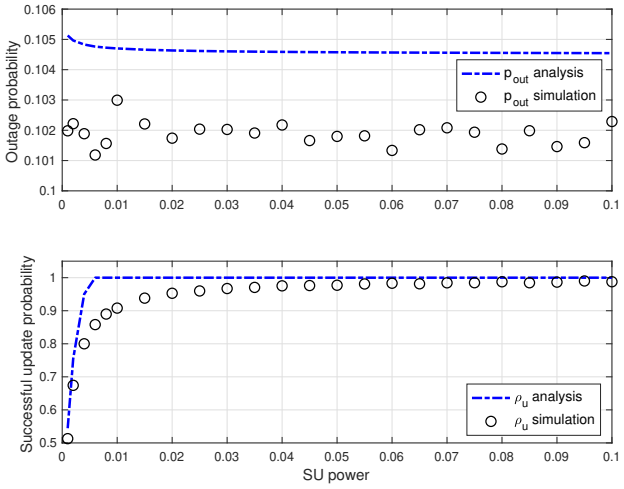

Figure 9. Probabilities vs. SU power with $\alpha = 4$, $r_{\mathrm{r}} = 2$, $P_{\mathrm{p}} = 0.1$, $\lambda_{\mathrm{p}} = 0.01$, $d_{\mathrm{p}} = d_{\mathrm{s}} = 1$.

with fixed density of PUs, $\lambda_{\mathrm{p}} = 0.005$. In the low power region, the average AoI decreases sharply as the successful update probability increases, and it achieves its minimum at $P_{\mathrm{s}} = 0.07$ even the successful update probability is low at about $\rho_{\mathrm{u}} = 0.35$, cf. Fig. 7. As the transmit power grows, the average AoI keeps increasing, which is dominated by the growth of the full charging time. The optimal transmit power can be obtained based on the analytical results accurately.

Fig. 8-9 show the results when varying SUs' power P_{s} with $\alpha = 4$, $r_{\mathrm{r}} = 2$, $P_{\mathrm{p}} = 0.1$, $\lambda_{\mathrm{p}} = 0.01$, $d_{\mathrm{p}} = d_{\mathrm{s}} = 1$. In all figures, the analytical results approximate the simulation results very well. Fig. 8 shows that the average AoI and the average full charging time are increasing monotonically as P_{s} grows since it takes longer to accumulate sufficient energy for a higher transmit power. In Fig. 9, we observe that the successful update probability grows quickly to 1 because d_{s} is small and the interference is low. The low power of SUs causes a weak impact on the primary network, thus, the outage probability decreases slightly as P_{s} increases.

VI. Conclusion

In this paper, we have studied a cognitive radio network with multiple users where SUs harvest wireless energy from PUs. The performance metric, AoI, has been adopted to evaluate the timeliness of status updates in the secondary network. The distributions of PUs and SUs have been modeled as point processes. In particular, PUs follows an HPPP and SUs

in the network are placed as a BPP with a fixed number. We have defined a greedy policy for status updates of SUs, which enables each battery charging cycle to be a renewal process. The average AoI of the secondary network has been characterized by deriving an upper and a lower bound. Simulation results verify that the gap of the upper and the low bound is small and the analytical result can serve as a proper approximation of the average AoI. Future work includes formalizing the performance of the greedy policy as compared to the optimal policy, and the development of online policies via reinforcement learning approaches.

Appendix A. Proof of Theorem 1

The proof follows a similar procedure in [32, Appendix B]. From (15), the outage probability can be written as

$$p_{\text{out}} = 1 - \Pr\Big(g_{x_\text{p}} \geq \frac{\theta_\text{p} d_\text{p}^\alpha}{P_\text{p}}(I_\text{p} + I_\text{s1} + \sigma^2)\Big) \tag{53}$$

$$= 1 - \mathbb{E}_{I_\text{p}}\Big[\mathbb{E}_{I_\text{s1}}\Big[\exp\Big(-\frac{\theta_\text{p} d_\text{p}^\alpha}{P_\text{p}}(I_\text{p} + I_\text{s1} + \sigma^2)\Big)\Big]\Big] \tag{54}$$

$$= 1 - \exp(-s_1\sigma^2)\mathbb{E}_{I_\text{p}}\big[\exp(-s_1 I_\text{p})\big]\mathbb{E}_{I_\text{s1}}\big[\exp(-s_1 I_\text{s1})\big] \tag{55}$$

where (54) follows from $g_{x_\text{p}} \sim \text{Exp}(1)$, (55) is due to the independency of I_p and I_s1, and $s_1 \triangleq \frac{\theta_\text{p} d_\text{p}^\alpha}{P_\text{p}}$. Note that $\mathbb{E}_{I_\text{p}}\big[\exp(-s_1 I_\text{p})\big]$ is the Laplace transform in terms of random variable I_p with input parameter s_1. Based on the result in [34, Sec. 5.1.7], we have

$$\mathbb{E}_{I_\text{p}}\big[\exp(-s_1 I_\text{p})\big] = \exp\Big(-\frac{\lambda_\text{p}\pi}{\text{sinc}(\frac{2}{\alpha})}(P_\text{p} s_1)^{\frac{2}{\alpha}}\Big). \tag{56}$$

Next, we derive $\mathbb{E}_{I_\text{s1}}\big[\exp(-s_1 I_\text{s1})\big]$ by following the result in [35, Lemma 4]. From (3), we have

$$\mathbb{E}_{I_\text{s1}}\big[\exp(-s_1 I_\text{s1})\big]$$

$$= \mathbb{E}\Big[\prod_{y\in\Phi_\text{s}} \exp\Big(-s_1 P_\text{s}\mathbb{1}_y g_y |y - x_0|^{-\alpha}\Big)\Big] \tag{57}$$

$$= \mathbb{E}\Big[\prod_{y\in\Phi_\text{s}} \frac{1}{1 + s_1 P_\text{s}\mathbb{1}_y |y - x_0|^{-\alpha}}\Big] \tag{58}$$

$$= \mathbb{E}\Big[\frac{1}{1 + s_1 P_\text{s}\mathbb{1}_y |y - x_0|^{-\alpha}}\Big]^{N_\text{s}} \tag{59}$$

$$= \Big(1 - \rho_\text{t} + \rho_\text{t}\phi_2\Big)^{N_\text{s}}, \tag{60}$$

where (58) is from the Laplace transform of exponential random variable g_y, (59) is by the independency of the placement of SUs, (60) is by taking the expectation of $\mathbb{1}_y$, and $\phi_2 \triangleq \mathbb{E}\Big[\frac{1}{1+s_1 P_\text{s}|y-x_0|^{-\alpha}}\Big]$. The conditional probability density function (PDF) of distance from a random point to a reference point v_0 given v_0 [35, Lemma 2] is

$$f_U(u|v_0) = \begin{cases} \frac{2u}{R^2}, & 0 \leq u \leq R - v_0, \\ \frac{2u}{\pi R^2}\arccos\big(\frac{u^2+v_0^2-R^2}{2uv_0}\big), & R - v_0 < u \leq R + v_0. \end{cases} \tag{61}$$

Since the distribution of PRs is also a HPPP, PRs are uniformly distributed in the considered area. The PDF of distance from a random PR to the origin [35] is

$$f_{v_0}(v) = \frac{2v}{R^2}. \tag{62}$$

Then, ϕ_2 in (60) can be calculated as

$$\phi_2 \triangleq \mathbb{E}\Big[\frac{1}{1 + s_1 P_\text{s}|y - x_0|^{-\alpha}}\Big]$$

$$= \int_0^R \int_0^{R+x_0} \frac{1}{1 + s_1 P_\text{s} u^{-\alpha}} f_U(u|x_0) f_{v_0}(x_0) du dx_0. \tag{63}$$

By substituting (56) and (60) into (55), we obtain the result in Theorem 1.

Appendix B. Proof of Lemma 1

Note that $P_\text{o}(t)$ are i.i.d. over slots. Then, by (10), we have

$$\mathbb{E}[P_\text{o}] = \mathbb{E}_{\mathcal{D}_2}\Big[\sum_{x\in\mathcal{D}_2}\bar{P}\Big] + \mathbb{E}_{\mathcal{D}_1}\Big[\mathbb{E}_{g_x}\Big[\sum_{x\in\mathcal{D}_1}\eta P_\text{p} g_x |x|^{-\alpha}\Big]\Big] \tag{64}$$

$$= \pi r_\text{r}^2 \lambda_\text{p}\bar{P} + \mathbb{E}_{\mathcal{D}_1}\Big[\sum_{x\in\mathcal{D}_1}\eta P_\text{p}|x|^{-\alpha}\Big] \tag{65}$$

$$= \pi r_\text{r}^2 \lambda_\text{p}\bar{P} + \frac{2\pi\lambda_\text{p}\eta P_\text{p}}{2-\alpha}\big(r_\text{h}^{2-\alpha} - r_\text{r}^{2-\alpha}\big). \tag{66}$$

The last equation is from the result of [34, Sec. 5.1.2]. For the variance of $P_\text{o}(t)$,

$$\text{Var}(P_\text{o}) = \text{Var}\Big(\sum_{x\in\mathcal{D}_2}\bar{P}\Big) + \text{Var}\Big(\sum_{x\in\mathcal{D}_1}\eta P_\text{p} g_x |x|^{-\alpha}\Big) \tag{67}$$

$$= \pi r_\text{r}^2\lambda_\text{p}\bar{P}^2 + 2\text{Var}\Big(\sum_{x\in\mathcal{D}_1}\eta P_\text{p}|x|^{-\alpha}\Big) + \mathbb{E}\Big[\sum_{x\in\mathcal{D}_1}\eta P_\text{p}|x|^{-\alpha}\Big]^2 \tag{68}$$

$$= \pi r_\text{r}^2\lambda_\text{p}\bar{P}^2 + \frac{2\pi\lambda_\text{p}\eta^2 P_\text{p}^2}{1-\alpha}\big(r_\text{h}^{2-2\alpha} - r_\text{r}^{2-2\alpha}\big) + \Big[\frac{2\pi\lambda_\text{p}\eta P_\text{p}}{2-\alpha}\big(r_\text{h}^{2-\alpha} - r_\text{r}^{2-\alpha}\big)\Big]^2, \tag{69}$$

where (67) is from the independency of $\mathcal{D}_1$ and $\mathcal{D}_2$, (68) is by the variance of the product of independent random variables g_x and $\mathcal{D}_1$, and (69) is from the result of [34, Sec. 5.1.3].

Appendix C. Proof of Lemma 2

By the total probability law, we have

$$\rho_\text{u} = \frac{\Pr(\gamma_\text{s} \geq \theta_\text{s}) - \Pr(\gamma_\text{s} \geq \theta_\text{s}|N_\text{g} > 0)\Pr(N_\text{g} > 0)}{\Pr(N_\text{g} = 0)} \tag{70}$$

$$\approx \frac{1}{\rho_\text{g}}\Pr(\gamma_\text{s} \geq \theta_\text{s}), \tag{71}$$

where the approximation is by setting $\Pr(\gamma_\text{s} \geq \theta_\text{s}|N_\text{g} > 0) \approx 0$. Since we consider $P_\text{p} \gg P_\text{s}$, it is reasonable to assume that an outage must occur even there is only one PR in the

guard zone of the SU [32, Appendix C]. Next, we focus on $\Pr(\gamma_{\rm s} \geq \theta_{\rm s})$. From (6), we have

$$\begin{aligned}
&\Pr(\gamma_{\rm s} \geq \theta_{\rm s}) \\
&= \Pr\Big(g_{y_{\rm s}} \geq \frac{\theta_{\rm s} d_{\rm s}^{\alpha}}{P_{\rm s}}(I_{\rm p} + I_{\rm s2} + \sigma^2)\Big) && (72)\\
&= \mathbb{E}_{I_{\rm p}}\Big[\mathbb{E}_{I_{\rm s2}}\Big[\exp\Big(-\frac{\theta_{\rm s} d_{\rm s}^{\alpha}}{P_{\rm s}}(I_{\rm p} + I_{\rm s2} + \sigma^2)\Big)\Big]\Big] && (73)\\
&= \exp(-s_2\sigma^2)\mathbb{E}_{I_{\rm p}}\big[\exp(-s_2 I_{\rm p})\big]\mathbb{E}_{I_{\rm s2}}\big[\exp(-s_2 I_{\rm s2})\big] && (74)
\end{aligned}$$

where (73) follows from $g_{y_{\rm s}} \sim \mathrm{Exp}(1)$, (74) is due to the independency of $I_{\rm p}$ and $I_{\rm s2}$, and $s_2 \triangleq \frac{\theta_{\rm s} d_{\rm s}^{\alpha}}{P_{\rm s}}$. Follow the same procedure in Appendix A, we have

$$\mathbb{E}_{I_{\rm p}}\big[\exp(-s_2 I_{\rm p})\big] = \exp\Big(-\frac{\lambda_{\rm p}\pi}{\mathrm{sinc}(\frac{2}{\alpha})}(P_{\rm p} s_2)^{\frac{2}{\alpha}}\Big). \quad (75)$$

$$\mathbb{E}_{I_{\rm s2}}\big[\exp(-s_2 I_{\rm s2})\big] = \Big(1 - \rho_{\rm t} + \rho_{\rm t}\beta_2\Big)^{N_{\rm s}-1}, \quad (76)$$

where

$$\begin{aligned}
\beta_2 &\triangleq \mathbb{E}\Big[\frac{1}{1 + s_2 P_{\rm s}\,|y - y_0|^{-\alpha}}\Big] \\
&= \int_0^R \int_0^{R+y_0} \frac{1}{1 + s_2 P_{\rm s} u^{-\alpha}} f_U(u|y_0) f_{v_0}(y_0) du dy_0.
\end{aligned} \quad (77)$$

By substituting (75) and (76) into (74), we obtain the result in Lemma 2.

REFERENCES

[1] A. Kosta, N. Pappas, V. Angelakis *et al.*, "Age of information: A new concept, metric, and tool," *Foundations and Trends® in Networking*, vol. 12, no. 3, pp. 162–259, 2017.

[2] S. Kaul, M. Gruteser, V. Rai, and J. Kenney, "Minimizing age of information in vehicular networks," in *Proc. 8th Annual IEEE Commun. Society Conf. on Sensor, Mesh and Ad Hoc Commun. and Networks (SECON)*, 2011, pp. 350–358.

[3] S. Kaul, R. Yates, and M. Gruteser, "Real-time status: How often should one update?" in *Proc. IEEE INFOCOM*, 2012, pp. 2731–2735.

[4] S. K. Kaul, R. D. Yates, and M. Gruteser, "Status updates through queues," in *Proc. 46th Annual Conference on Information Sciences and Systems (CISS)*, 2012.

[5] I. Kadota, E. Uysal-Biyikoglu, R. Singh, and E. Modiano, "Minimizing the age of information in broadcast wireless networks," in *Proc. 54th Annual Allerton Conference on Communication, Control, and Computing (Allerton)*, 2016, pp. 844–851.

[6] A. M. Bedewy, Y. Sun, and N. B. Shroff, "Age-optimal information updates in multihop networks," in *Proc. IEEE Intern. Sympos. on Inf. Theory*, 2017, pp. 576–580.

[7] Y. Sun, E. Uysal-Biyikoglu, R. D. Yates, C. E. Koksal, and N. B. Shroff, "Update or wait: How to keep your data fresh," *IEEE Trans. Inf. Theory*, vol. 63, no. 11, pp. 7492–7508, 2017.

[8] J. Zhong, E. Soljanin, and R. D. Yates, "Status updates through multicast networks," in *Proc. 55th Annual Allerton Conference on Communication, Control, and Computing (Allerton)*, 2017, pp. 463–469.

[9] J. Zhong, R. D. Yates, and E. Soljanin, "Multicast with prioritized delivery: How fresh is your data?" in *Proc. 19th International Workshop on Signal Processing Advances in Wireless Communications (SPAWC)*, 2018, pp. 1–5.

[10] R. D. Yates and S. K. Kaul, "The age of information: Real-time status updating by multiple sources," *IEEE Trans. Inf. Theory*, vol. 65, no. 3, pp. 1807–1827, 2019.

[11] Y.-P. Hsu, E. Modiano, and L. Duan, "Age of information: Design and analysis of optimal scheduling algorithms," in *Proc. IEEE Intern. Sympos. on Inf. Theory*, 2017, pp. 561–565.

[12] I. Kadota, A. Sinha, E. Uysal-Biyikoglu, R. Singh, and E. Modiano, "Scheduling policies for minimizing age of information in broadcast wireless networks," *IEEE/ACM Transactions on Networking*, vol. 26, no. 6, pp. 2637–2650, 2018.

[13] A. M. Bedewy, Y. Sun, S. Kompella, and N. B. Shroff, "Age-optimal sampling and transmission scheduling in multi-source systems," *arXiv preprint arXiv:1812.09463*, 2018.

[14] J. Zhong, W. Zhang, R. D. Yates, A. Garnaev, and Y. Zhang, "Age-aware scheduling for asynchronous arriving jobs in edge applications," in *Proc. IEEE INFOCOM WKSHPS*, 2019.

[15] R. D. Yates, "Lazy is timely: Status updates by an energy harvesting source," in *Proc. IEEE Intern. Sympos. on Inf. Theory*, 2015, pp. 3008–3012.

[16] B. T. Bacinoglu, E. T. Ceran, and E. Uysal-Biyikoglu, "Age of information under energy replenishment constraints," in *Proc. IEEE Inf. Theory Workshop*, 2015, pp. 25–31.

[17] B. T. Bacinoglu and E. Uysal-Biyikoglu, "Scheduling status updates to minimize age of information with an energy harvesting sensor," in *Proc. IEEE Intern. Sympos. on Inf. Theory*, 2017, pp. 1122–1126.

[18] A. Arafa and S. Ulukus, "Age-minimal transmission in energy harvesting two-hop networks," in *Proc. IEEE Global Commun. Conf.*, 2017.

[19] X. Wu, J. Yang, and J. Wu, "Optimal status update for age of information minimization with an energy harvesting source," *IEEE Trans. Green Commun. and Networking*, vol. 2, no. 1, pp. 193–204, 2018.

[20] A. Arafa, J. Yang, S. Ulukus, and H. V. Poor, "Age-minimal transmission for energy harvesting sensors with finite batteries: Online policies," *arXiv:1806.07271*, 2018.

[21] A. Baknina, O. Ozel, J. Yang, S. Ulukus, and A. Yener, "Sending information through status updates," in *Proc. IEEE Intern. Sympos. on Inf. Theory*, 2018.

[22] A. Baknina and S. Ulukus, "Coded status updates in an energy harvesting erasure channel," in *Proc. 52nd Annual Conference on Information Sciences and Systems (CISS)*, 2018.

[23] S. Feng and J. Yang, "Age of information minimization for an energy harvesting source with updating erasures: With and without feedback," *arXiv preprint arXiv:1808.05141*, 2018.

[24] X. Zheng, S. Zhou, Z. Jiang, and Z. Niu, "Closed-form analysis of non-linear age-of-information in status updates with an energy harvesting transmitter," *arXiv preprint arXiv:1906.00192*, 2019.

[25] Y. Dong, Z. Chen, and P. Fan, "Uplink age of information of unilaterally powered two-way data exchanging systems," in *Proc. IEEE INFOCOM WKSHPS*, 2018, pp. 559–564.

[26] I. Krikidis, "Average age of information in wireless powered sensor networks," *IEEE Commun. Lett.*, vol. 8, no. 2, pp. 628–631, 2019.

[27] Z. Chen, N. Pappas, E. Björnson, and E. G. Larsson, "Age of information in a multiple access channel with heterogeneous traffic and an energy harvesting node," *arXiv preprint arXiv:1903.05066*, 2019.

[28] A. Kosta, N. Pappas, A. Ephremides, and V. Angelakis, "Age of information and throughput in a shared access network with heterogeneous traffic," in *Proc. IEEE Global Commun. Conf.*, 2018.

[29] S. Leng and A. Yener, "Age of information minimization for an energy harvesting cognitive radio," *IEEE Trans. Cognitive Commun. and Networking*, vol. 5, no. 2, pp. 427–439, 2019.

[30] ——, "Minimizing age of information for an energy harvesting cognitive radio," in *Proc. IEEE Wireless Commun. and Networking Conf.*, 2019.

[31] ——, "Impact of imperfect spectrum sensing on age of information in energy harvesting cognitive radios," in *Proc. IEEE Intern. Commun. Conf.*, 2019.

[32] S. Lee, R. Zhang, and K. Huang, "Opportunistic wireless energy harvesting in cognitive radio networks," *IEEE Trans. Wireless Commun.*, vol. 12, no. 9, pp. 4788–4799, 2013.

[33] E. Demarchou, C. Psomas, and I. Krikidis, "Asynchronous ad hoc networks with wireless powered cognitive communications," *IEEE Trans. Cognitive Commun. and Networking*, vol. 5, no. 2, pp. 440–451, 2019.

[34] M. Haenggi, *Stochastic Geometry for Wireless Networks*. Cambridge University Press, 2012.

[35] M. Afshang and H. S. Dhillon, "Fundamentals of modeling finite wireless networks using binomial point process," *IEEE Trans. Wireless Commun.*, vol. 16, no. 5, pp. 3355–3370, 2017.

[36] E. Boshkovska, D. W. K. Ng, N. Zlatanov, and R. Schober, "Practical non-linear energy harvesting model and resource allocation for SWIPT systems," *IEEE Commun. Lett.*, vol. 19, no. 12, pp. 2082–2085, 2015.